Nucleic Acids Research, 1993, Vol. 21, No. 22 ***5005–5011***

Deuteriation of sugar protons simplify NMR assignments and structure determination of large oligonucleotide by the *^{1}H-NMR window* approach

S.-I.Yamakage, T.V.Maltseva, F. P.Nilson, A.Földesi and J.Chattopadhyaya*
Department of Bioorganic Chemistry, Box 581, Biomedical Center, University of Uppsala, S-751 23 Uppsala, Sweden

Received August 25, 1993, Revised and Accepted September 30, 1993

ABSTRACT

The concept of the *^{1}H-NMR window* has been developed and examined through a comparative study of NOESY spectra of a self-complementary Dickerson's dodecamer (I) [5′d(^{5}C^{6}G^{7}C^{8}G^{9}A^{10}A^{11}T^{12}T^{13}C-^{14}G^{15}C^{16}G)$_2$3′], a self-complementary 20-mer (II) [(^{5}′d(^{1}C^{2}G^{3}C^{4}G^{5}C^{6}G^{7}C^{8}G^{9}A^{10}A^{11}T^{12}T^{13}C^{14}G^{15}C^{16}G^{17}C-^{18}G^{19}C^{20}G)$_2$3′] in which the core part consists of the same Dickerson's dodecamer sequence with the flanking CGCG residues at both 3′ and 5′-ends, and the partly-deuteriated (shown by underlined CGCG residues at both 3′ and 5′-ends) analogous duplex (III) [5′d(^{1}C^{2}G^{3}C^{4}G^{5}C^{6}G^{7}C^{8}G^{9}A^{10}A^{11}T^{12}T^{13}C^{14}G^{15}C^{16}G^{17}C-^{18}G^{19}C ^{20}G)$_2$3′] in which the core ^{5}C to ^{16}G part (*i.e. ^{1}H-NMR window)* consists of the natural Dickerson's dodecamer sequence. A comparison of their NOESY spectra clearly demonstrates that the severe overlap of proton resonances in the larger DNA duplex (II) has been successfully reduced in the partly-deuterated duplex (III) as a result of specific incorporations of the sugar-deuteriated nucleotide residues in the latter [stereospecific >97 atom % ^{2}H enrichment at H2′, H2″ and H3′ sites, ~85 atom % ^{2}H enrichment at H4′ and ~20 atom % ^{2}H enrichment at H1′ (see refs. 10 and 11) in the 20-mer duplex (III)]. These simplifications of the resonance overlap by the deuteriation approach have enabled unequivocal chemical shift assignments and extraction of the quantitative NOE data in the ^{1}H-NMR window part of duplex (III). A comparison of the 12-nucleotide long ^{1}H-NMR window in (III) with that of the 12-mer duplex (I) also shows the scope of studying the changes in conformation and dynamics of the core 12-mer region in (III) which result from the increase of molecular weight due to the DNA chain extension. It is noteworthy that such a study is clearly impossible for the natural 20-mer (II) because of the inherent problem of the overlap of resonances.

INTRODUCTION

The conformational studies of large functional DNA and RNA molecules in solution are important to understand how the conformational characteristics and the variations of the local structure of these macromolecules translate into specific interaction and recognition that culminate into specific biological function. Nuclear Magnetic Resonance (NMR) spectroscopy has emerged as one of most powerful tools to understand the stereochemistry of interactions, recognitions and dynamics of both global and local structure variations. In the complex approach to solve the solution geometry of oligo-DNA or oligo-RNA molecules, NMR measurements provide the informations on bond torsion angles and interproton distances as inputs for the computational calculations for molecular model building. In an effort to collect these primary conformational informations, it is ideal that all resonance lines and cross-peaks due to interacting nuclei are clearly separated in homonuclear proton-proton, heteronuclear proton-carbon, proton-phosphorus, carbon-phosphorus, NOESY and ROESY experiments. This greatly facilitates an unambiguous assignment of all interacting protons. This in turn allows the determination of scalar couplings and interproton distances between pairs of relaxing protons from 2D nuclear Overhauser enhancement (NOESY) spectroscopy with a high degree of confidence and accuracy.

Despite the enormous developments both in hardwares (increasing magnetic field, more powerful computers) and spectral editing methods (1,2,3), present state-of-the-art NMR technologies allow us only partly to tackle the problem of spectral complexity due to the resonance overlap. It is possible to extract $^3J_{HH}$ and nOe volumes for only up to 14–16 mer duplex DNA in an unambiguous manner, but it is simply impossible to collect all of these informations in a non-prejudicial manner from a larger DNA molecule. Clearly, these problems are associated with spectral overlap which becomes more and more complex due to overcrowding of resonances, particularly from the repeating pentose moieties, with increasing chain length. The problem due to the severe spectral overlap of proton resonances in absorption

* To whom correspondence should be addressed

assignments and in measurements of $^3J_{HH}$ and nOe volume of a larger biologically functional DNA or RNA molecule could be tackled by substituting proton (^1H) with deuteron (^2H) chemically in a chosen domain and extracting the necessary information arising from the shorter NMR-visible non-deuteriated part (*^1H-NMR window*) (10,11). By incremental shift of the *^1H-NMR window* in a series of DNA or RNA oligomers with identical sequence (Fig. 1), it should be possible to put together the total structural information of a much larger oligonucleotide than what is possible today. The most important part in this concept is that two ^{1}H-NMR windows in two oligomers of the series (Fig. 1) should have at least an overlap of a nucleotide residue with specific chemical shifts in order to be able to correlate protons from both windows with respect to the same nucleotide reference point (*i.e.* same proton resonances in both NMR windows). Our approach of specific deuteriation of sugar residues (10,11) and their specific incorporation into the selected parts of oligo-DNA should allow us to probe the geometry of the short stretch of the core part in a larger DNA duplex which would help us to understand how the structure and dynamics of a specific core part of a DNA duplex changes as the DNA duplex chain becomes longer! We herein report our study of NOESY spectra of a self-complementary Dickerson's dodecamer (I) [5′d(^{5}C^{6}G^{7}C^{8}G^{9}A^{10}A^{11}T^{12}T^{13}C^{14}G^{15}C^{16}G)$_2$3′], a self-complementary 20-mer (II) [(5′d(^{1}C^{2}G^{3}C^{4}G^{5}C^{6}G^{7}C^{8}G^{9}A^{10}A^{1}T^{12}T^{3}C-^{14}G^{15}C^{16}G^{17}C^{18}G^{19}C^{20}G)$_2$3′] in which the core part consists of the same Dickerson's dodecamer sequence with the flanking CGCG residues at both 3′ and 5′-ends, and the partly-deuteriated (shown by underlined CGCG residues at both 3′ and 5′-ends) analogous duplex (III) [5′d(^{1}C^{2}G^{3}C^{4}G^{5}C^{6}G^{7}C^{8}G^{9}A^{10}A^{11}T^{12}T^{13}C-^{14}G^{15}C^{16}G^{17}C^{18}G^{19}C^{20}G)$_2$3′] in which the core ^{5}C to ^{16}G part (*i.e. ^1H-NMR window*) consists of Dickerson's dodecamer sequence. A comparison of their NOESY spectra clearly demonstrates the simplification achieved as a result of specific incorporations of the sugar-deuteriated nucleotide residues in partly-deuteriated 20-mer duplex (III). The accompanying manuscript also shows how does the local core structure becomes significantly flexible as the DNA duplex becomes larger. This has been explored by examining the detailed local dynamic properties of the imino-protons in the above DNA duplexes.

MATERIALS AND METHODS

Synthesis and sample preparation

Duplexes (I) 5′d(G^{5}C^{6}G^{7}C^{8}G^{9}A^{10}A^{11}T^{12}T^{13}C^{14}G^{15}C^{16}G)$_2$3′, (II) 5′(d^{1}C^{2}G^{3}C^{4}G^{5}C^{6}G^{7}C^{8}G^{9}A^{10}A ^{11}T^{12}T^{13}C^{14}G^{15}C^{16}G^{17}C^{18}G^{19}C^2 ^{0}G)$_2$3′ and (III) partly-deuteriated (shown by underline) counterpart 5′d(^{1}C^{2}G^{3}C^{4}G^{5}C^{6}G^{7}C^{8}G^{9}A^{10}A^{11}T^{12}T^{13}C^{14}G^{15}C^{16}G-^{17}C^{18}G^{19}C^{20}G)$_2$3′ were synthesized by phosphoramidite chemistry (4) using both natural and sugar-deuteriated (10, 11) (underlined) building blocks of 3′-β-cyanoethylphosphoamidite (5) of DMTr-A^{bz}, DMTr-G^{ibu}, DMTr-G^{dpc}ac, DMTr-C^{bz}, DMTr-C^{bz}, DMTr-T. The sugar-deuteriated phosphoramidite blocks have the following level of ^{2}H incorporations (10, 11): >97 atom % ^{2}H at C2′, C3′, C5/5′; ~85 atom % ^{2}H at C4′; ~20 atom % ^{2}H at C1′. Oligomer synthesis was performed (eight times 1.3 μmol scale synthesis) by Gene assembler Plus DNA sythesizer (Pharmacia-Kabi). After completion of the synthesis, the 5′-O-DMTr group of oligo-DNA was removed by acid treatment on the support, then the support was suspended in 32% ammonia-water (20 ml) at the ambient temparature for 7 days to cleave off the oligo-DNA as well as to remove benzoyl (bz), isobutyryl (ibu), acetyl (ac), diphenylcarbamoyl (dpc) and cyanoethyl protecting groups. After removal of ammonia gas from the reaction mixture by evaporation, the residual aqueous solution was washed with diethylether, then centrifuged, decanted and evaporated. The crude DNA mixture was purified using the analytical and preparative HPLC conditions as outlined below.

Purification of 12-mer duplex (I) and 20-mer DNA duplexes (II), and (III)

Analytical and preparative purification was carried out using Hplc (Waters™ 625 LC System: System controller Waters 600E, Pump, Tunable absorbance Detector Waters 486). Protein-Pak™ Q 8HR 1000 Å was used for analytical and preparative runs. The crude mixture was purified under denaturing conditions [buffer (1): 0. 01M NaOH (pH 12), buffer (2): 1M NaCl, 0.01M NaOH (pH 12)]. The system was operated using a linear gradient of 55−70% of buffer (2) over a period of 30 min with a loading of 50 o.d units of crude DNA mixture per injection. Appropriate fractions were pooled and desalted by using Sephadex G-25 (Super fine DNA grade). Finally, purified sample (240 o.d units, 10.3 %) was lyophilized to dryness from D_2O (99.9%D atom).

Nuclear magnetic resonance spectroscopy

The above lyophilized sample was dissolved in 0.4 ml of the following buffer for NMR measurements 200 mM NaCl, 20 mM NaD_2PO_4, 20μM EDTA, pH 7.0 in D_2O (99.98%D atom). ^{1}H-NMR spectra were recorded on a Bruker AMX−500 NMR spectrometer (^{1}H at 500 MHz). To calculate the rates of exchange and life-times of the imino protons of the duplexes (I)−(III) the combination NOESY and ROESY experiments approach (6) has been used. Phase-sensitive NOESY experiments (7) were performed at 294 K using the following parameters: mixing time 0.2 s, 4K complex data points in t_2, 512 complex data points in t_1, a relaxation delay of either 2.0 or 10 s, a sweep width of 5050.5 Hz in both dimensions, 128 acquisitions per FID and a shifted sine-square bell apodization function for both dimensions. The data were zero-filled in t_1 to give 4K×1K complex data points. The residual water resonance was saturated during the relaxation delay. NOE cross-peak volumes were measured using the program AURELIA (8) with segmentation level 0.5 and 1000 iterations. Two-dimensional data sets for DQF-COSY (9) spectra were collected in the phase-sensitive mode with the time-proportional phase incrementation with and without phosphorus decoupling. Typically 4096 data points were collected for each 512 t_1 values in DQF-COSY experiments. The 512×4096 data points were resolution enhanced by a shifted squared sine-bell window function in both the t_1 and t_2 directions, then Fourier transformed and phase adjusted. A 90° pulse width of 12.25 μs with relaxation delay of either 2s or 10s was used. The data were collected with the nonspinning sample to avoid t_1 noise.

RESULTS AND DISCUSSION

The effect of stereospecific (10,11) >97 atom % ^{2}H enrichment at H2′, H2″ and H3′ sites, ~85 atom % ^{2}H enrichment at H4′ and ~20 atom % ^{2}H enrichment at H1′ in 20-mer duplex (III) is clearly evident (Figs. 2−5) through the comparison of its 12-nucleotide long *^1H-NMR window* at the core part with the natural 20-mer counterpart (II). A comparison of the 12-nucleotide long *^1H-NMR window* in (III) with that of the 12-mer duplex (I), which constitute the core part in 20-mer (III),

also shows the scope of studying the conformation and dynamics of the core 12-mer region in (III) as a result of the extension of the DNA sequence in (I) by CGCG residues in the tail and the head part. The assignment and the chemical shifts of aromatic (H6/H8/H5/CH_3) and sugar protons (H1′, H2′, H2″, H3′ and H4′) for all three duplexes have been presented in Table 1. A comparison of the chemical shifts of the core part (from ^{5}C to ^{16}G) shows the proton absorptions of residues at the 3′- and 5′-ends (^{5}C, ^{6}G and ^{7}C at 5′-end and ^{16}G, ^{15}C and ^{14}G at 3′-end) of the dodecamer duplex (I) are generally more relatively deshielded than the protons of the corresponding residues in 20-mer duplexes (II) and (III), which is expected due to the dangling ends in duplex (I). One other important point of interest is that the chemical shifts of all observable protons in 20-mer (II) and its deuteriated counterpart (III) are only very slightly different ($\geq \pm 0.02$ ppm) (10,11) which means that there is no significant deuterium isotope effect on the chemical shifts as a result of incorporations of deuteriated sugars in oligo-DNA. The structural integrities of the duplexes (I), (II) and (III) are easily assessed by the presence of all expected cross-peaks between aromatic H8/H6 and the anomeric H1′ proton of the sugar moiety (Fig. 2) for each constituent nucleotide residue present in the duplexes.

A comparison of the H8/H6-H1′ cross-peaks that arise from the core 12-mer sequence (from ^{5}C to ^{16}G) (Fig. 2) in the non-deuteriated 20-mer (II) and in the *^{1}H-NMR window* part of the partly-deuteriated 20-mer (III) duplexes also allows the estimation of the NOE volumes, which have been directly compared with that of the Dickerson's dodecamer sequence (I) *(vide infra)*. The expanded regions showing cross-peaks between aromatic and H1′

Table 1. Chemical shifts of the aromatic H8/H6/H5/CH_3 and anomeric H1′, H2′, H2″, H3′ and H4′ protons of duplexes (I), (III) and (III)

Residue	Duplex	H8/H6	H5/CH_3	H1'	H2'	H2"	H3'	H4'
^{1}C	(I)	**	**	**	**	**	**	**
	(II)	7.74	6.01	5.86	2.07	2.51	4.81	4.46
	(III)	7.73	6.01	5.84	*	*	*	*
^{2}G	(I)	**	**	**	**	**	**	**
	(II)	8.07		6.00	2.64	2.78	5.08	4.81
	(III)	8.06		5.99	*	*	*	*
^{3}C	(I)	**	**	**	**	**	**	**
	(II)	7.43	5.49	5.82	2.12	2.50	4.91	4.29
	(III)	7.42	5.49	5.80	*	*	*	*
^{4}G	(I)	**	**	**	**	**	**	**
	(II)	7.99		5.97	2.71	2.81	5.07	4.44
	(III)	7.97		5.96	*	*	*	*
^{5}C	(I)	7.72	5.99	5.84	2.05	2.49	4.79	4.15
	(II)	7.36	5.43	5.74	2.04	2.43	4.91	4.24
	(III)	7.35	5.41	5.72	2.04	2.44	4.92	4.22
^{6}G	(I)	8.04		5.98	2.76	2.81	5.06	4.44
	(II)	7.94		5.91	2.66	2.75	5.04	4.42
	(III)	7.92		5.91	2.65	2.75	5.03	4.41
^{7}C	(I)	7.36	5.46	5.68	1.93	2.36	5.06	4.22
	(II)	7.28	5.38	5.59	1.85	2.29	4.86	4.16
	(III)	7.27	5.37	5.59	1.86	2.30	4.85	4.16
^{8}G	(I)	7.95		5.53	2.73	2.86	5.09	4.41
	(II)	7.91		5.49	2.71	2.82	5.05	4.38
	(III)	7.90		5.48	2.71	2.81	5.05	4.37
^{9}A	(I)	8.20		6.09	2.79	3.03	5.16	4.55
	(II)	8.18		6.05	2.76	3.00	5.14	4.53
	(III)	8.17		6.05	2.77	3.00	5.13	4.53
^{10}A	(I)	8.21		6.25	2.65	3.02	5.11	4.56
	(II)	8.19		6.23	2.63	3.00	5.10	4.54
	(III)	8.19		6.22	2.63	2.99	5.08	4.54
^{11}T	(I)	7.20	1.35	6.00	2.07	2.66	4.91	4.30
	(II)	7.19	1.32	5.98	2.06	2.61	4.90	4.28
	(III)	7.20	1.33	5.98	2.05	2.64	4.91	4.28
^{12}T	(I)	7.46	1.62	6.19	2.25	2.64	4.99	4.30
	(II)	7.44	1.59	6.17	2.23	2.62	4.98	4.28
	(III)	7.43	1.59	6.16	2.23	2.62	4.97	4.28
^{13}C	(I)	7.56	5.71	5.75	2.15	2.50	4.97	4.24
	(II)	7.52	5.67	5.72	2.12	2.48	4.95	4.22
	(III)	7.52	5.66	5.70	2.13	2.48	4.94	4.22
^{14}G	(I)	8.00		5.94	2.71	2.76	5.08	4.45
	(II)	7.96		5.93	2.68	2.70	5.06	4.43
	(III)	7.95		5.92	2.66	2.78	5.07	4.44
^{15}C	(I)	7.42	5.53	5.84	1.99	2.41	5.09	4.25
	(II)	7.37	5.41	5.73	2.04	2.44	5.06	4.42
	(III)	7.36	5.41	5.72	2.13	2.48	5.05	4.42
^{16}G	(I)	8.03		6.24	2.45	2.69	4.77	4.55
	(II)	7.97		5.94	2.71	2.80	5.06	4.44
	(III)	7.97		5.93	2.70	2.79	5.05	4.44
^{17}C	(I)	**	**	**	**	**	**	**
	(II)	7.38	5.45	5.76	2.06	2.41	4.97	4.29
	(III)	7.37	5.44	5.74	*	*	*	*
^{18}G	(I)	**	**	**	***	**	**	**
	(II)	7.98		5.95	2.73	2.77	5.07	4.45
	(III)	7.98		5.94	*	*	*	*
^{19}C	(I)	**	**	**	**	**	**	**
	(II)	7.42	5.55	5.85	1.98	2.42	4.89	4.24
	(III)	7.41	5.54	5.84	*	*	*	*
^{20}G	(I)	**	**	**	**	**	**	**
	(II)	8.03		6.25	2.71	2.46	4.77	4.27
	(III)	8.03		6.24	*	*	*	*

*Signal is absent due to deuteriation in duplex (III).
**These residues are absent for the Dickerson's dodecamer (I).

protons have been presented for the non-deuteriated 20-mer (II) in Fig. 2A, partly-deuteriated 20-mer (III) in Fig. 2B and Dickerson's 12-mer (I) in Fig. 2C. A preliminary inspection of Figs 2A and 2B shows that the H8/H6-H1′ regions in both the spectra of the 20-mers look very similar, but the comparison of the NOE spectra of both 20-mers (Figs 2A/2B) with that of the 12-mer (Fig. 2C) shows that the chemical shifts of the three terminal residues at 3′- and 5′-ends of the 12-mer (I) are considerably different (see Table 1). The intranucleotidyl and internucleotidyl distances between H8/H6-H1′ protons have been estimated using the two protons approximation methodology, $r_{ij}6 = r_{ref}6\sigma_{ij}/\sigma_{ref}$ (where r_{ij} is the unknown distance between protons i and j and r_{ref} is the reference distance of H6-H5 protons in cytosine, σ_{ij} and σ_{ref} are the cross relaxation rate constants between the corresponding protons). The data show that under the present experimental condition (*i.e.* 200 mM NaCl, 20 mM NaD_2PO_4, 20 μM EDTA, pH 7.0 at 21°C) the intranucleotidyl distances, H8/$H6_k$-H1′$_k$ (for k-residue), and the internucleotidyl distances, H1′$_{k-1}$-H8/$H6_k$, are similar for the corresponding protons in all three duplexes within experimental accuracy. This suggests that the structure of the core part (from ^{8}G to ^{13}C) in all three duplexes in the above buffer system are comparable.

A further comparison of H8/H6-H1′ regions between duplexes (II) and (III) shows that the intensity of the H8/H6-H1′ cross-peaks for the H1′ of the partly-deuteriated sugar residues are enhanced and the line- width decreased (Fig. 2B). The following phenomenona are responsible for this: **(1)** The decrease of the line-width of H1′ of the deuteriated sugar residue is partly due to the increase of its T_2 relaxation time due to the difference in the nuclear magnetic properties of deuterium in the H2′, H2″ and H3′ positions (12) compared with hydrogen. **(2)** The absence of vicinal H1′-H2′/H2″ J-couplings (10, 11, 13) in deuteriated sugar moieties has also contributed to the enhancements of H8/H6-H1′ cross-peaks. **(3)** Finally, the enhancements of the intensity of H8/H6-H1′ cross-peaks are also partly due to the reduced number of pathways of relaxation (14, 15) of H1′ proton in the partly-deuteriated sugar. The result of these cumulative

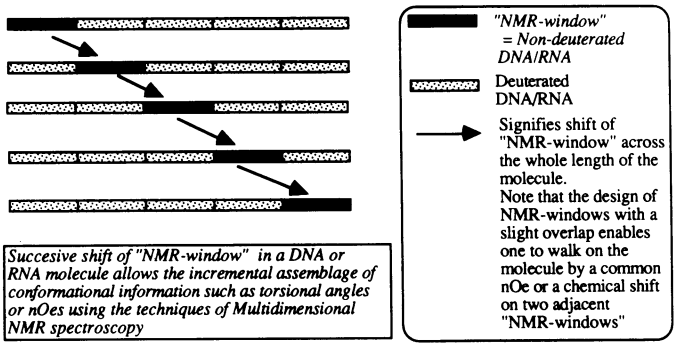

Figure 1. The '*^{1}H-NMR window*' concept for determination of local structure of large oligo-DNA or -RNA (see refs. 10 and 11).

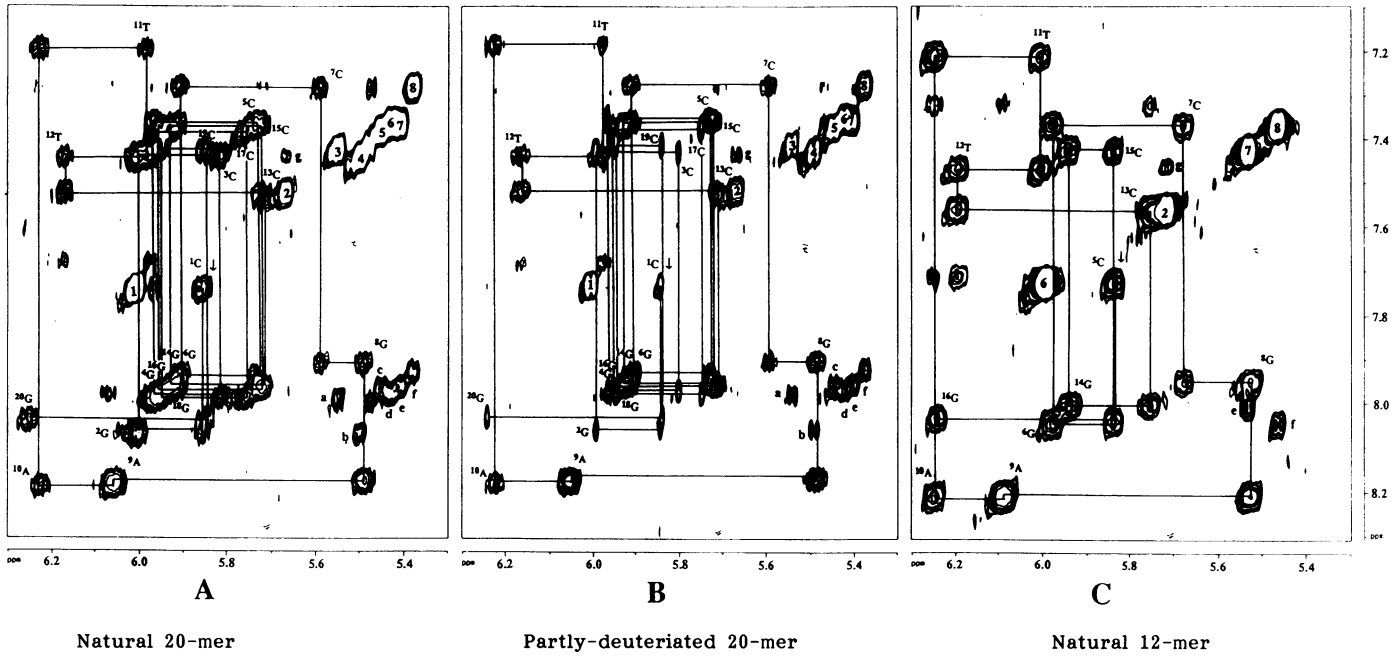

Figure 2. Expanded NOESY spectrum of the aromatic to H1′ regions of natural 20-mer (II), its partly-deuteriated 20-mer derivative (III) and a 12-mer (I): Panel **(A)** shows a self-complementary 20-mer duplex (II) in which the core part (^{5}C to ^{16}G) consists of the same Dickerson's dodecamer sequence residues with the flanking CGCG sequence at both 3′- and 5′-ends. Panel **(B)** shows partly-deuteriated derivative of the 20-mer duplex (III) and a panel **(C)** shows the 12-mer dodecamer (I). The eight strong pyrimidine H5 to H6 cross-peaks are the most intense ones, which are also identified through DQF-COSYspectra (data not shown); and are labelled by arabic numbers in parenthesis from (1) to (8): (1) ^{1}C(H6, H5, (2) ^{13}C(H6, H5), (3) ^{19}C(H6, H5), (4) ^{3}C(H6, H5), (5) ^{17}C(H6, H5), (6) ^{5}C(H6, H5), (7) ^{15}C(H6, H5) and (8) ^{7}C(H6, H5). The sequential connectivity from the 5′-end (^{1}C) (labelled by arrow) to the 3′-end (^{20}G) is connected by solid lines. Only the intraresidual cross-peaks are labelled. The cross-peaks between C_{k+1}(H5)-G_k(H8) are marked by letters (a) to (g): (a) ^{19}C(H5)-^{18}G(H8), (b) ^{3}C(H5)-^{2}G(H8), (c) ^{17}C(H5)-^{16}G(H8), (d) ^{5}C(H5)-^{4}G(H8), (e) ^{15}C(H5)-^{14}G(H8), (f) ^{7}C(H5)-^{6}G(H8) and also (g) ^{13}C(H5)-^{12}T(H6). NOESY spectra collected at 200 ms mixing time at 21°C (see experimental section).

effects can be easily detected qualitatively upon inspection of the corresponding H8/H6-H1′ cross-peaks in the NOESY spectra of both partly-deuteriated sugars and non-deuteriated sugars in 20-mer (III) (Fig. 2B) and this is also apparent by comparison of the H8/H6-H1′ cross-peaks of the deuteriated sugar in duplex (III) with those of the corresponding non-deuteriated sugars in duplex (II) (compare for instance the H8-H1′ cross-peak of the partly-deuteriated ^{20}G residue in which it is sharper than in non-deuteriated ^{10}A residue). This unique enhancements of H8-H1′ cross-peaks of the partly-deuteriated residues can be used as powerful tool for discrimination between H8/H6 and H1′ protons in deuteriated and non-deuteriated sugar residues in a partly-deuteriated duplex (Fig. 2B).

Significant simplification of the aromatic H8/H6-H2′, H2″; H8/H6-H3′ and H1′-H2′, H2″ protons in the 2D NOESY spectrum of the partly-deuteriated 20-mer (III), relative to the non-deuteriated 20-mer (II), has been also observed (Figs. 3–5). For the partly-deuteriated duplex (III), the assignement of the H2′, H2″ protons in the *^{1}H-NMR window* could be easily achieved by starting from the ^{5}C(H6) protons (labelled by an arrow in Fig. 3B), which has been identified using the H8/H6-H1′ cross-peak region. Subsequently, all cross-peaks from ^{5}C to ^{16}G residue due to 'through-space' NOESY connectivities along the H2′/H2″$_{(i-1)}$ → H8/H6$_{(i)}$ → H2′/H2″$_{(i)}$ pathway (Fig. 3B) have been assigned. These assignements have been unambiguously confirmed (Fig. 4B) using the NOE connectivities of H1′-H2′/H2″ region (δ5.2–6.4 ppm in F2 direction and δ1.7–3.2 ppm in F1 direction) in which only the cross-peak between H1′-H2′/2″ of the non-deuteriated sugar have been observed. The situation is dramatically changed for the non-deuteriated duplex (II) (Fig. 3A) in which the H2′, H2″ protons could not be unambiguously assigned without taking the help of the chemical shift assignments of the 12-mer part in the *^{1}H-window* in duplex (III) (Fig. 3B). The effect of the selective nucleotide deuteriation is nicely illustrated through a comparison of the NOE cross-peaks between H8/6-H2′/2″ region in Fig. 3A and 3B (box). Four terminal G-C base pairs in both 3′- and 5′-termini of the duplexes (II) and (III) were specially chosen in order to establish the advantages of the present deuteriation approach for more complex overlaping cross-peaks in the NOESY spectra. In Fig. 3B (box), *four sets of guanine cross-peaks* from H8-H2′/H2″ protons of ^{6}G, ^{8}G, ^{14}G and ^{16}G residues of duplex (III) are only found as a result of specific deuteriation of 3′- and 5′-terminal CGCG residues, whereas the NOESY spectrum of the corresponding region in duplex (II) shows [Fig. 3A (box)] *eight sets of guanine cross-peaks* arising from ^{2}G, ^{4}G, ^{6}G, ^{8}G, ^{14}G, ^{16}G, ^{18}G and ^{20}G residues which all severely overlap. It is noteworthy that the complexity due to the overlap of these four sets of NOE cross-peaks from H8-H2′/H2″ protons of ^{6}G, ^{8}G, ^{14}G and ^{16}G residues in deuteriated 20-mer (III) is quite comparable to the corresponding cross-peaks in 12-mer (I), which is marked by a box in Fig. 3C. In Fig. 4, a similar effect is also noted in the cross-peak of H1′-H2′/ H2″ [highlighted in boxes (a) and (b) in Fig. 4] when ^{2}G, ^{4}G, ^{18}G and ^{20}G residues were deuteriated in duplex (III). As a result of the selective deuteriation of the sugar residues of ^{2}G, ^{4}G, ^{18}G and ^{20}G in duplex (III), it has been possible to quantitatively calculate the volume of cross-peaks arising from the intraresidual G_k(H1′)-G_k(H2′, H2″) NOEs [shown in box (a)] and the inter-residual C_{k+1}(H5)–G_k(H2′, H2″) NOEs [shown in box (b)].

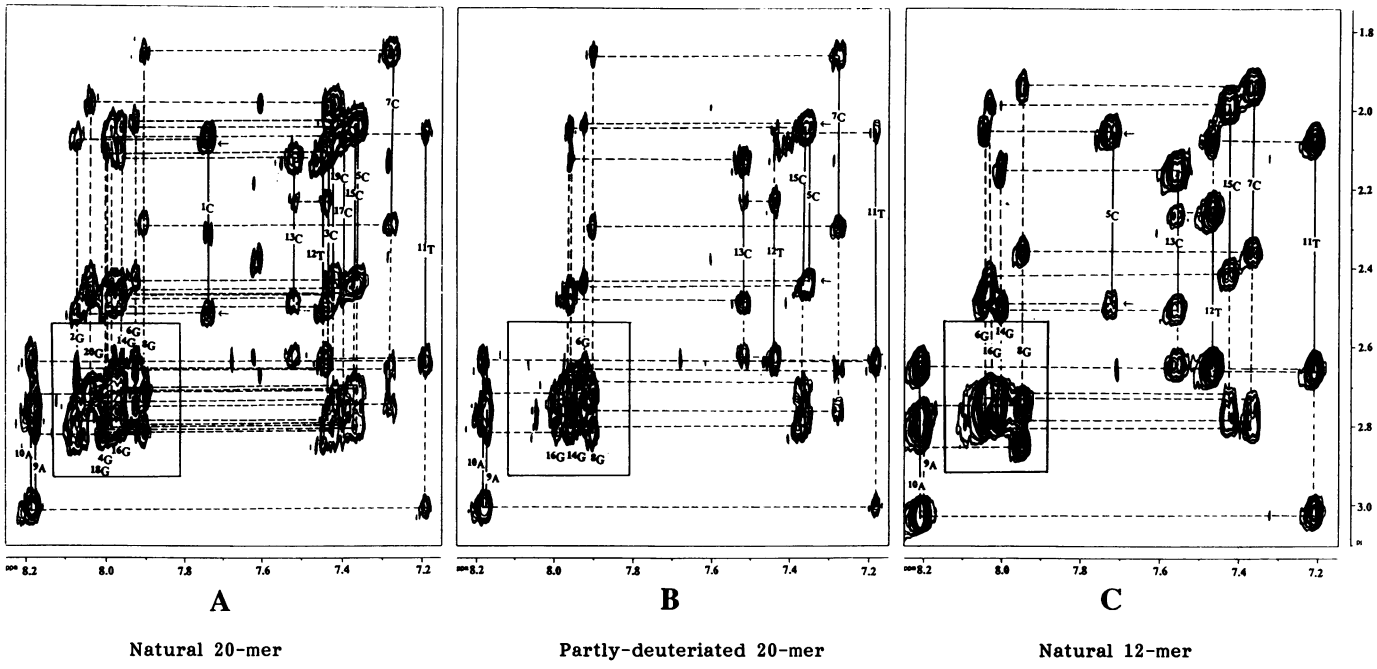

Figure 3. Expanded NOESY spectrum of the aromatic to H2′/H2″/CH$_3$ region of natural 20-mer (II), its partly-deuteriated 20-mer derivative (III) and a 12-mer (I): Panel **(A)** shows the duplex (II). Panel **(B)** shows partly-deuteriated duplex (III) and Panel **(C)** shows the 12-mer duplex (I). The sequential connectivity was also traced as in the aromatic to H1′ region, shown in Fig. 1, with the help of the analysis of H1′ to H2′ region from the ^{1}C nucleotide at the 5′-end (labelled by arrow) to ^{20}G at the 3′-end. The intraresidual cross-peaks between aromatic to H2′/H2″ are connected by horizontal solid lines and labelled. The cross-peaks from the aromatic to the n–1 H2′/H2″ are connected to the (n–1) intraresidual cross-peaks between aromatic to H2′/H2″ by vertical dashed lines. The intraresidual cross-peaks between aromatic to H2′/H2″ of the ^{2}G, ^{4}G, ^{6}G, ^{8}G, ^{14}G, ^{16}G, ^{18}G and ^{20}G residues are highlighted in the box at the left hand corner of the spectra.

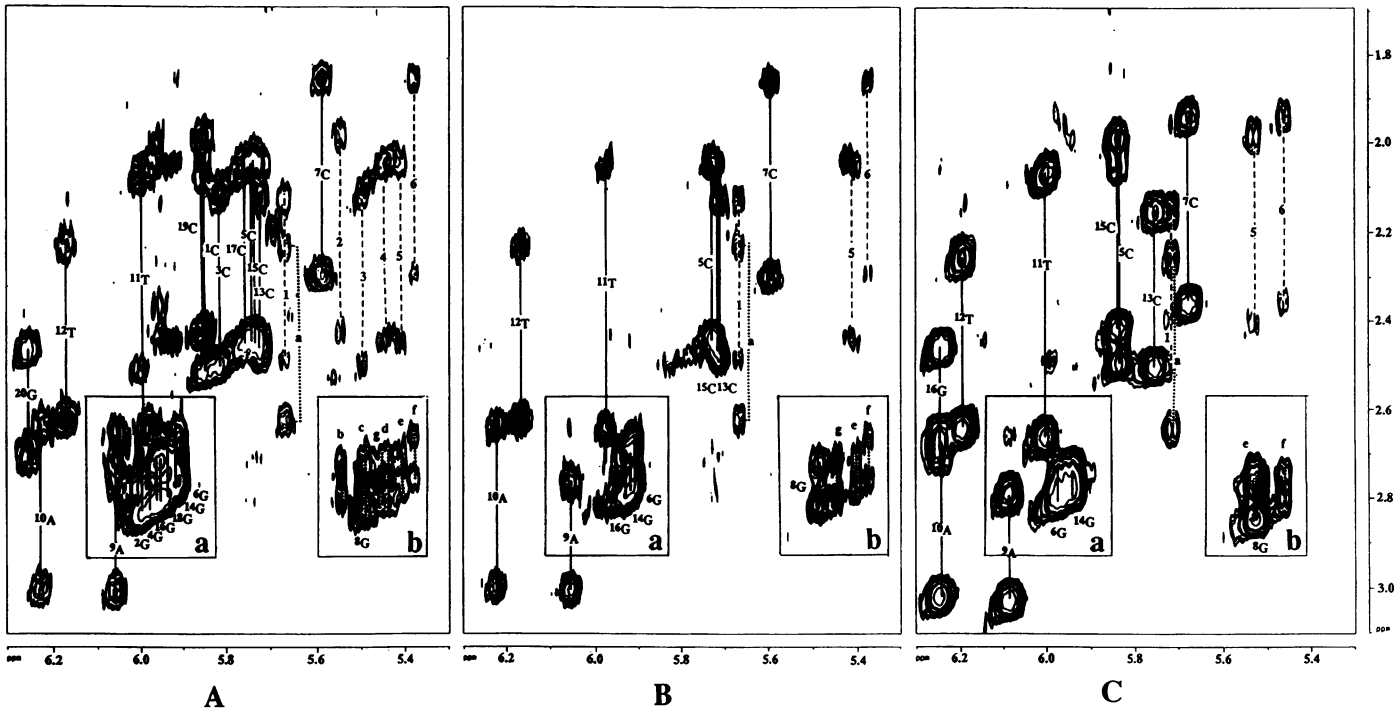

Figure 4. Expanded NOESY spectrum of the H1′ to H2′/H2″ region of natural 20-mer (II), its partly-deuterated 20 mer derivative (III) and a 12-mer (I): Panel **(A)** shows the 20-mer duplex (II). Panel **(B)** shows partly-deuteriated 20-mer duplex (III) and Panel **(C)** shows the 12-mer duplex (I). The intraresidual cross-peaks between H1′ to H2′/H2″ are connected by vertical solid lines and labelled. The cross-peaks from the aromatic C(H5) to H2′/H2″ of the same residue are connected by the dashed lines and labelled by arabic from (1) to (6): (1) ^{13}C(H5, H2′/H2″), (2) ^{19}C(H5, H2′/H2″), (3) ^{3}C(H5, H2′/H2″), (4) ^{5}C(H5, H2′/H2″), (5) ^{15}C(H5, H2′/H2″), (6) ^{7}C(H5, H2′/H2″). The cross-peaks from the aromatic C(H5) to the (n−1) G(H2′/H2″) are highlighted in the box [box (b)] at the right hand corner of the spectra. They are connected by vertical dotted line and labelled by (a) to (g): (a) ^{13}C(H5)-^{12}T(H2′/H2″), (b) ^{19}C(H5)-^{18}G(H2′/H2″), (c) ^{3}C(H5)-^{2}G(H2′/H2″), (d) ^{5}C(H5)-^{4}G(H2′/H2″), (e) ^{15}C(H5)-^{14}G(H2′/H2″), (f) ^{7}C(H5)-^{6}G(H2′/H2″), (g) ^{17}C(H5)-^{16}G(H2′/H2″). The intraresidual cross-peaks between H1′ to H2′/H2″ of the ^{2}G, ^{4}G, ^{6}G, ^{8}G, ^{14}G, ^{16}G and ^{18}G residues are highlighted in a box [box (a)] at the left hand corner of the spectra.

In addition, it may be also seen that several closely spaced cross-peaks between H8/H6 and H3′ protons in the NOESY spectrum of the non-deuteriated duplex (II) essentially complicate this region (Fig. 5A) compared to the corresponding part in the partly-deuteriated duplex (III) (Fig. 5B). In particular, the almost identical chemical shifts of the cross-peaks between H8/H6 and H3′ protons of ^{5}C, ^{15}C, ^{17}C, ^{19}C, ^{3}C, ^{13}C, ^{12}T and ^{4}G, ^{18}G, ^{14}G, ^{16}G, ^{8}G, ^{6}G residues (Fig. 5A) in the duplex (II) make it completely impossible to extract the NOEs between H8/H6 and H3′ protons, which are necessary to define their glycosyl torsions in an unambiguous manner. In contrast, such overcrowdings of cross-peaks of H8/H6 and H3′ protons in the partly-deuteriated duplex (III) for the corresponding ^{5}C, ^{15}C, ^{13}C, ^{12}T, 8G and ^{6}G residues (Fig. 5B) have been considerably simplified, which are all well resolved and are indeed observed separately (except for ^{14}G, ^{16}G cross-peaks which overlap with each other). This is why they could be successfully used for NOE volume calculations with a high degree of accuracy and confidence. Note that the simplfication of overlap achieved in the region of cross-peaks between H8/H6 and H3′ protons of ^{5}C, ^{15}C, ^{13}C, ^{12}T, ^{8}G and ^{6}G residues (Fig. 5B) in partly-deuteriated duplex (III) are now quite comparable, as expected, to the corresponding cross-peaks from the 12-mer duplex (Fig. 5C). These data clearly show that the *^{1}H-NMR window* approach is reasonably successful for achieving simplification of the resonance overlap problem in the proton spectrum of large oligo-DNA. This enables the assignment

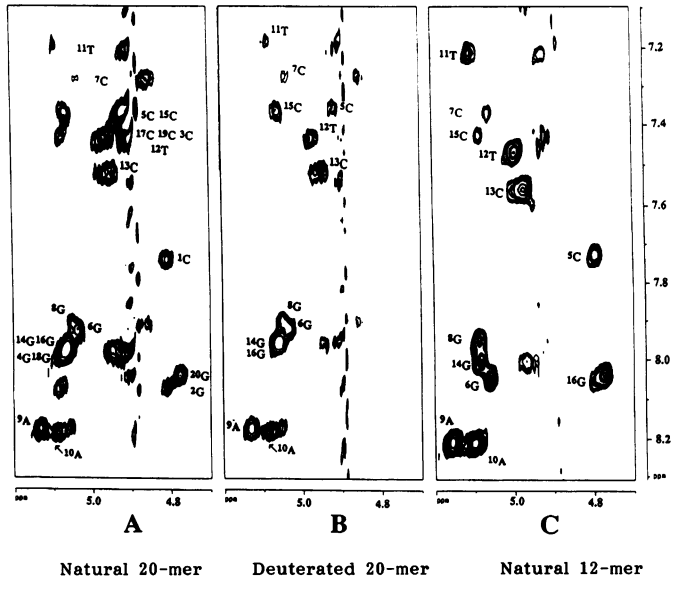

Figure 5. Expanded NOESY spectrum of the aromatic to H3′/H4′ region of 20-mer (II), its partly-deuteriated 20-mer derivative (III) and a 12-mer (I): Panel **(A)** shows the natural 20-mer duplex (II). Panel **(B)** shows partly-deuteriated 20-mer duplex (III) and Panel **(C)** shows the 12-mer duplex (I) The intraresidual cross-peaks between aromatic to H3′/H4′ are labelled by the residue and number.

of the proton resonances of larger DNA duplex more completely than what has been possible hithertofore. It also allows the extraction of the quantitative NOE data from otherwise overlaping part of the spectrum. The work is in progress in this laboratory to show that such in *^{1}H-NMR window* approach is indeed useful to perform conformational analysis of biologically functional genes provided their relaxation properties and the solubilities do not become acute problem.

ACKNOWLEDGEMENTS

The authors wish to thank the Swedish Board for Technical Development (NUTEK), the Swedish Natural Science Research Council (NFR) and Wallenbergstiftelsen for generous financial support.

REFERENCES

1. Hosur, R. V., Govil, G. and Miles, H. T. (1988) *Magn. Reson. Chem.* **26**, 927–944.
2. (a) Ernst, R. R., Bodenhausen, G. and Wokaun, A. *Principles of Nuclear Magnetic Resonance in One and Two Domensions*, Clarendon Press: Oxford, 1987. (b) Oppenheimer, N. J., James, T. L. Eds. (1989) *Methods Enzymol.*, **176**, Chapter 1 & 2.
3. (a) Vuister, G.W. and Boelens, R. (1987) *J. Magn. Reson.*, **73**, 328–333. (b) Mooren, M. M. W., Hilbers, C. W., Van Der Marel, G. A., Van Boom, J. H. and Wijmenga, S. S. (1991) *J. Magn. Reson.*, **94**, 101–111. (c) Majumdar, A. and Hosur, R. V. (1991) *J. Biomol. NMR*, **1**, 205–208. (d) Sörensen, O. W. (1990) *J. Magn. Reson.* , **90**, 433- 438.
4. McBride, L. J. and Caruthers, M. H. (1983) *Tetrahedron Lett*, **24**, 245–248.
5. Sinha, N. D., Biernat, J., McManus, J. and Köster, H. (1984) *Nucleic Acid Res.*, **12**, 1539–1558.
6. Maltseva, T.V, Yamakage, S.-I, Agback, P. and Chattopadhyaya, J. (1993) *Nucleic Acid Res.* **18**, 4288–4295; Nucleic Acid Res. 18, 4246–4252;.
7. Bodenhausen, G., Kogler, H. and Ernst, R. R. (1984) *J. Magn. Reson.*, **580**, 370–383.
8. Program AURELIA was supplied by BRUKER Spectrospin.
9. Neuhaus, D., Wagner, G., Vasak, M., Kagi, J. H. R. and Wuthrich, K. (1985) *Eur. J. Biochem.*, **151**, 257–273.
10. Földesi, A., Nilson, F. P. R., Glemarec, C., Gioeli, C. and Chattopadhyaya, J. (1992) *Tetrahedron*, **48**, 9033–9072.
11. Földesi, A., Nilson, F. P. R., Glemarec, C., Gioeli, C. and Chattopadhyaya, J. (1993) *J. Biochem. Biophis. Methods*, **26**, 1–26.
12 Agback, P, Maltseva, T.V, Nilson, F. P. R., Földesi, A. and Chattopadhyaya, J. Manuscript in preparation
13. Oda, Y., Nakamura, H., Yamazaki, T., Nagayama, K., Yoshida, M., Kanaya, S. and Ikehara, M. (1992) *J. Biomolecular NMR*, **2**, 137–147.
14. Pachter, R., Arrowsmith, C. H. and Jardetzky, O. (1992) *J. Biomolecular NMR*, **2**, 183–194.
15. Keepers, J. W. and James, T.L. (1982) *J. Am. Chem. Soc.* **104**, 929–939.